PHASE FIELD MODELS, ADAPTIVE MESH REFINEMENT AND LEVEL SETS FOR SOLIDIFICATION PROBLEMS

Nigel Goldenfeld

Department of Physics
University of Illinois at Urbana-Champaign

COWORKERS AND COLLABORATORS

- Phase-field calculations
  - ◇ Jon Dantzig (UIUC, Mechanical and Industrial Engineering)
  - ◇ Nikolas Provatas (now at Paprican)
  - ◇ Jun-Ho Jeong (UIUC, M&IE)
  - ◇ Yung-Tae Kim (UIUC, Physics)
- Experimental work
  - ◇ Martin Glicksman (RPI, MatSE)
  - ◇ Matthew Koss (Holy Cross, Physics)
  - ◇ Jeffrey LaCombe (UN-Reno, MatSE)
  - ◇ Afina Lupulescu (RPI, MatSE)
- Funding from NASA, NSF, DARPA

INTRODUCTION

- Motivation
  - ◇ Dendrites are generic microstructural feature in metals and alloys
  - ◇ Pattern set by solidification determines properties
  - ◇ Processing conditions determine microstructure
- Mathematical and computational issues
  - ◇ Complex free boundary problem: front tracking and imposition of boundary conditions are hard to do, because numerical instabilities and physical instabilities get coupled
  - ◇ Multiple length and time scale resolution required
  - ◇ Large computation times

PHENOMENOLOGY: PURE MATERIALS

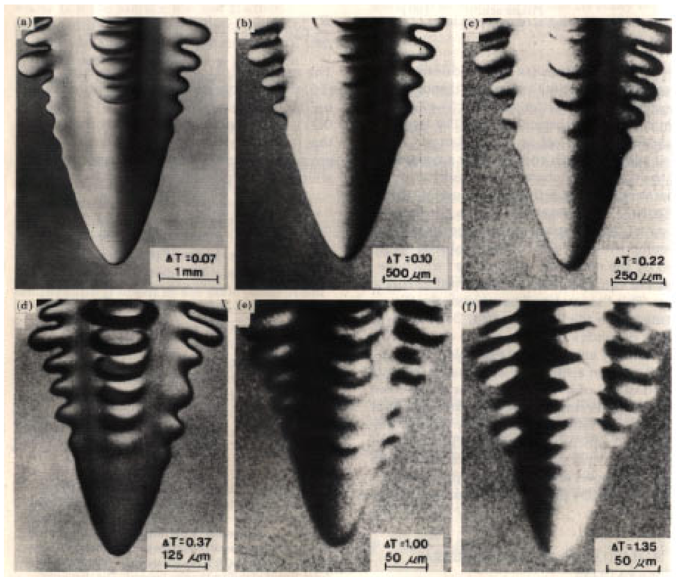

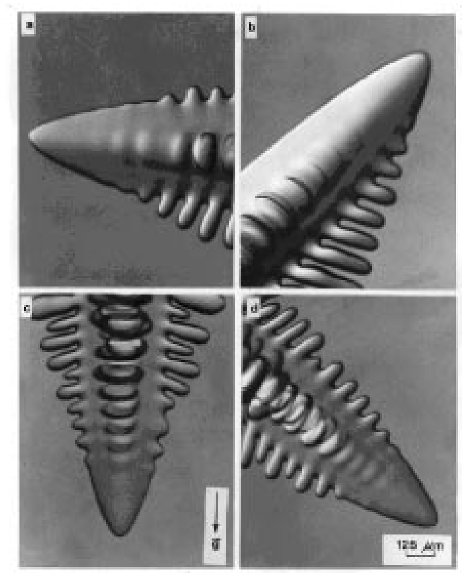

- Experiments by Glicksman, et al.
- High purity succinonitrile (SCN) growing into an undercooled melt
- Left photographs show that length scale determined by bulk undercooling

A BRIEF HISTORY OF DENDRITE SOLIDIFICATION THEORY

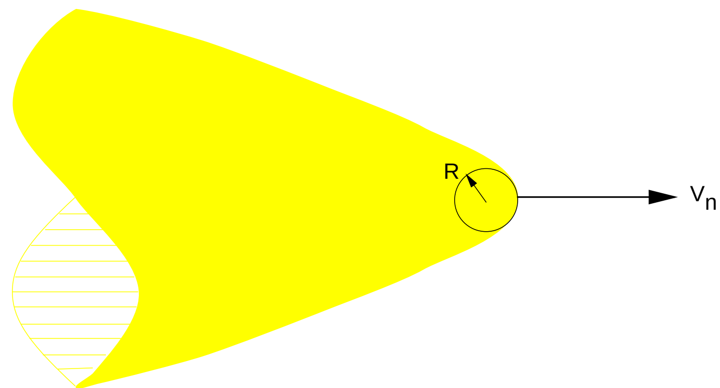

- Ivantsov (1948): Diffusion controlled growth of a parabaloidal needle crystal into an undercooled melt at T_∞
  - ◇ Shape preserving, steady growth at velocity V_n and tip radius R
  - ◇ Interface is an isotherm at temperature T_m

$$Iv\underbrace{\left(\frac{V_n R}{2\alpha}\right)}_{Pe} = \frac{T_m - T_\infty}{L_f/c_p} = \Delta T$$

  - ◇ "Operating state" is not uniquely determined
  - ◇ Shape is unstable at all wavelengths

HISTORY OF DENDRITE SOLIDIFICATION THEORY (cont'd)

- Temkin (1960): Surface tension modifies the interface boundary condition

$$T = T_m - \frac{\sigma}{\Delta S_f}\kappa = T_m - \Gamma\kappa$$

$$\frac{T - T_m}{L_f/c_p} = -\frac{\Gamma}{L_f/c_p}\kappa = -d_0\kappa$$

  - ◇ Γ is Gibbs-Thomson coefficient
  - ◇ d_0 is capillary length, $\mathcal{O}\left(10^{-8}\text{m}\right)$
  - ◇ Suggests that this produces a maximum velocity for a single R

- Glicksman: Careful experiments in SCN and P show that this extremum value is not the operating state

- Nash & Glicksman (1974): Boundary integral method to compute dendrite shape and dynamics. Still doesn't agree with experiments

HISTORY OF DENDRITE SOLIDIFICATION THEORY (cont'd)

- Langer, Müller-Krumbhaar, others: Marginal stability hypothesis

$$R \sim \sqrt{d_0(D/V_n)}$$

$$V_n R^2 = \sigma^* d_0 D$$

  - ◇ $\sigma^* = 1/4\pi^2$ seems to agree with experiments for SCN

- Ben-Jacob et al. & Kessler et al. (1984): solvability theory
  - ◇ Nash-Glicksman equation has no solutions: need to add surface tension anisotropy, e.g.,

$$\sigma = \sigma_0(1 + \epsilon \cos 4\theta)$$

  - ◇ Solve Nash-Glicksman integral equation
  - ◇ Discrete set of solutions, rather than continuous
  - ◇ Only stable solution corresponds to operating state

THE PHASE-FIELD METHOD FOR SOLIDIFICATION

- Basic idea
  - ◇ Continuous auxiliary field that regularises the solidification front with width W
  - ◇ Coupled equations for physical + auxiliary variables reproduce sharp interface model as $W \to 0$
- Introduce *phase-field* on a fixed grid
  - ◇ $\phi = -1$ corresponds to liquid, $\phi = +1$ to solid
  - ◇ Define interface position as $\phi = 0$

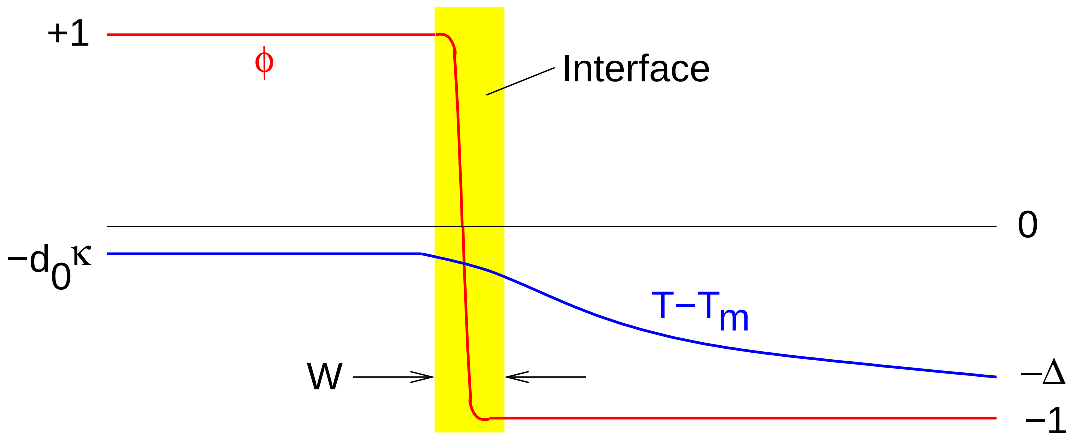

PHYSICAL INTERPRETATION OF THE PHASE-FIELD

- The phase field has no genuine or unique physical interpretation: nor needs one!
- Can think of it as being coarse-grained entropy density (e.g. Warren and Boettinger)

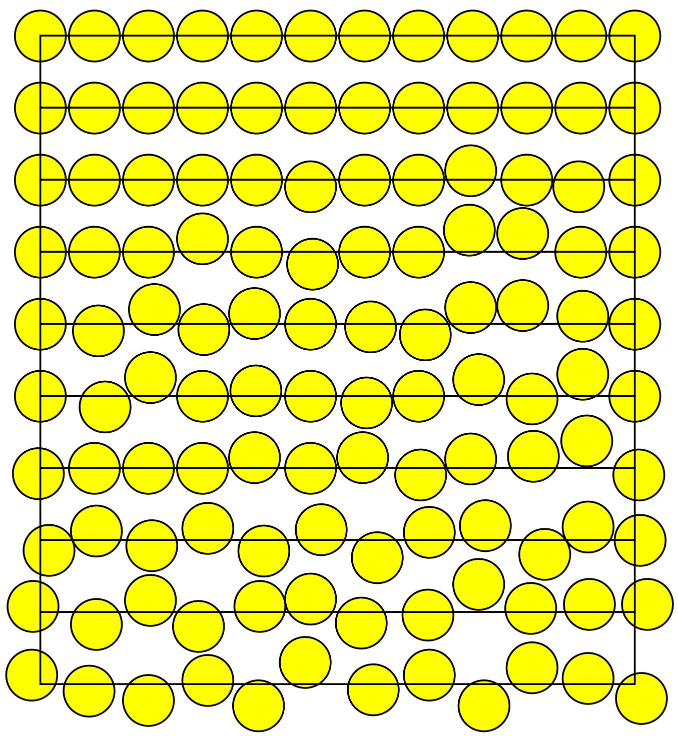

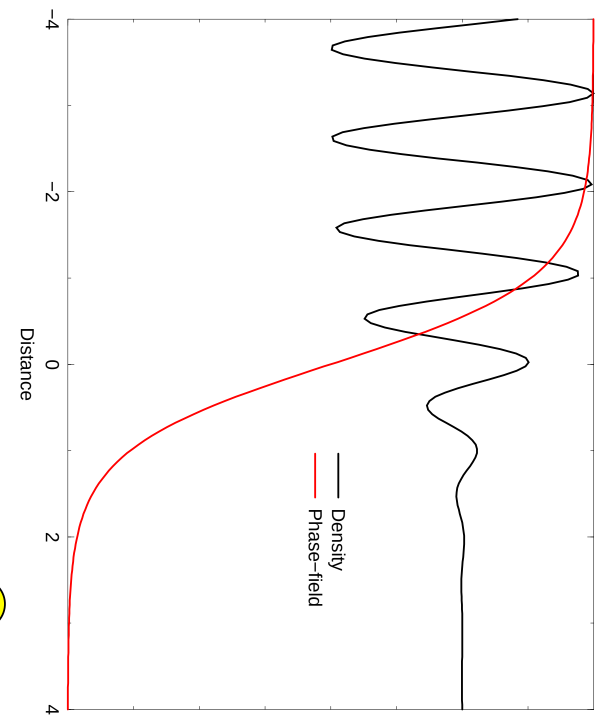

PHASE-FIELD MODEL FOR A PURE MATERIAL

- Diffuse interface of thickness W, defined by a *phase-field* ϕ

$$\rho c_p \frac{\partial T}{\partial t} = \nabla \cdot (k \nabla T) + \frac{L_f}{2} \frac{\partial \phi}{\partial t}$$

$$\tau \frac{\partial \phi}{\partial t} = -\frac{\delta \mathcal{F}}{\delta \phi}$$

  - ◇ Attributes: thin interface, $\phi = \pm 1$ as stable states

$$\mathcal{F} = \int_{\mathrm{vol}} \left(\frac{1}{2} |w(\vec{n}) \nabla \phi|^2 + f(\phi, T) \right) d^d \vec{x}$$

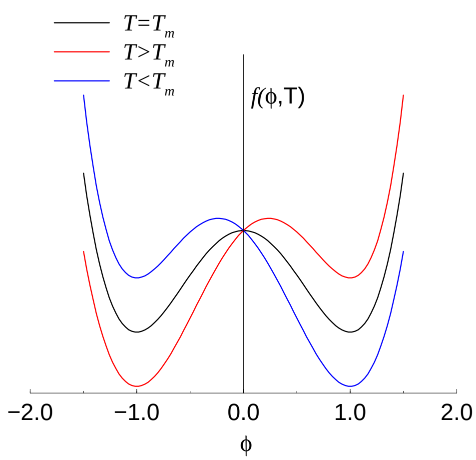

HIERARCHY OF LENGTH SCALES

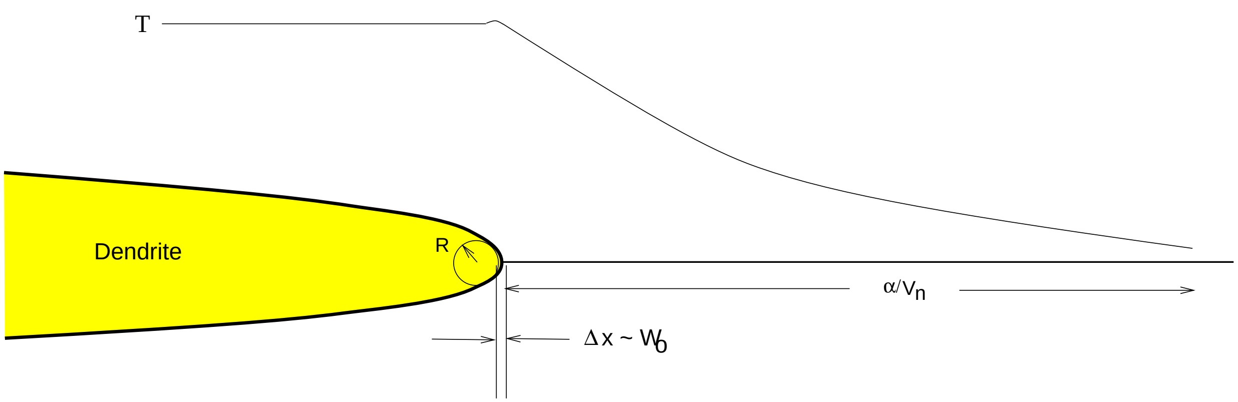

- Length scales: d_0, α/V_n, R, W_0, Δx, L_B
  - ◇ Convergence requires $\Delta x \sim \mathcal{O}(W_0)$
  - ◇ Asymptotics set $W_0 \sim d_0$ (10^{-8} m)
  - ◇ Domain independence requires $L_B \sim \mathcal{O}(\alpha/V_n)$ (10^{-4} m)
  - ◇ Uniform mesh requires $N_g = (L_B/\Delta x)^d$ (10^8 in 2-D)
- Result is long computation time for all ΔT
  - ◇ Many experiments are at low ΔT: diffusion length $\alpha/V_n \gg R$

PRACTICAL PHASE FIELD CALCULATIONS: IMPROVED ASYMPTOTICS

- Phase field calculations were essentially impractical until two separate technical improvements were made:
  - ◇ Improved asymptotics to relate phase field parameters to those of the underlying sharp interface model
  - ◇ Adaptive mesh refinement to minimize computational complexity
- Karma showed that one can use a “thin-interface” analysis in which $d_0 \ll W \ll$ pattern size but the equations still mimic the sharp interface limit
- Specific parameters can be eliminated from the sharp interface model by judicious choice of the phase field parameters
  - ◇ Kinetics: allows thermal dendrites to be simulated
  - ◇ Temperature jump, correction to the Stefan condition, surface diffusion: allow two-sided diffusion to be simulated

PRACTICAL PHASE FIELD CALCULATIONS: ADAPTIVE MESH REFINEMENT IN 2D

- All phase field calculations can be improved by selectively placing computational nodes in the rapidly varying interface region
- Initial uniform mesh of 4-noded quadrilateral elements
- Refinement/fusion based on $f(\nabla\phi, \nabla U)$
- Data structure
  - ◇ Use of linked lists and quadtrees makes element traversal efficient
  - ◇ Extra side nodes resolved with triangular elements

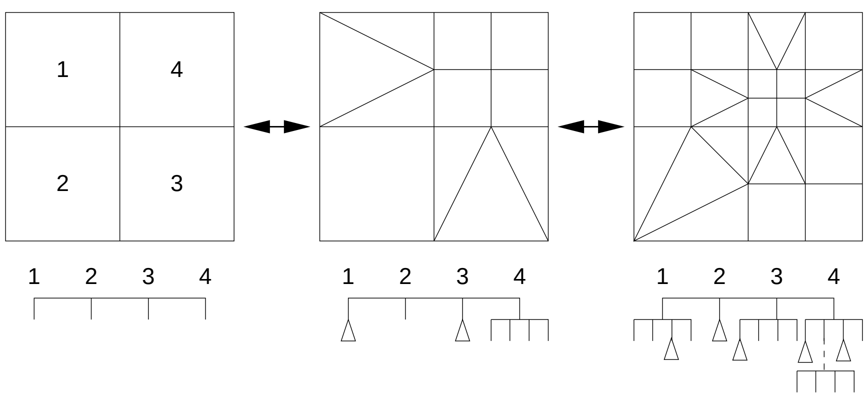

ISOLATED DENDRITE AT HIGH UNDERCOOLING

- Adaptive grid tracks boundary
- Temperature solution looks like boundary layer
- Tip speed and shape match solvability theory

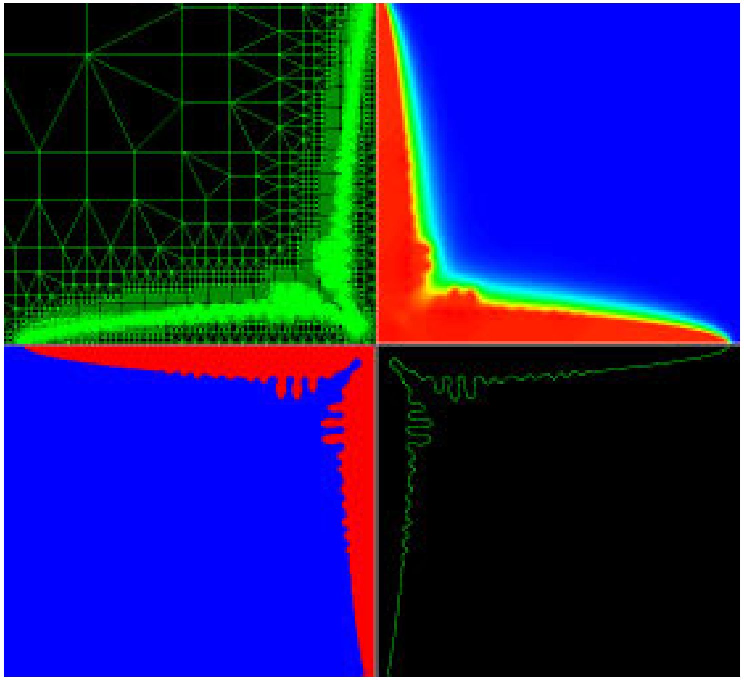

UNIVERSALITY OF PHASE FIELD MODEL PREDICTIONS

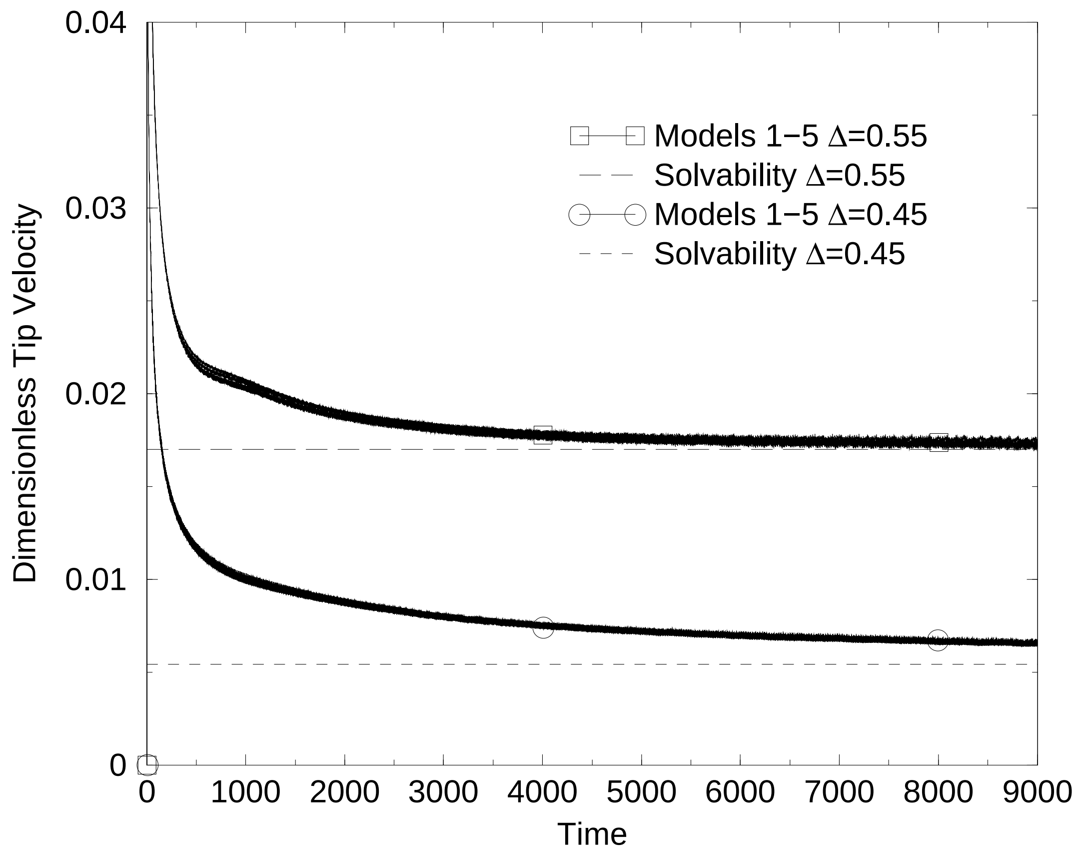

- We tested that using a variety of different phase field models, properly computed and converged gave exactly the same time dependence and steady state behaviour

BREAKDOWN OF PHASE FIELD MODEL ASYMPTOTICS

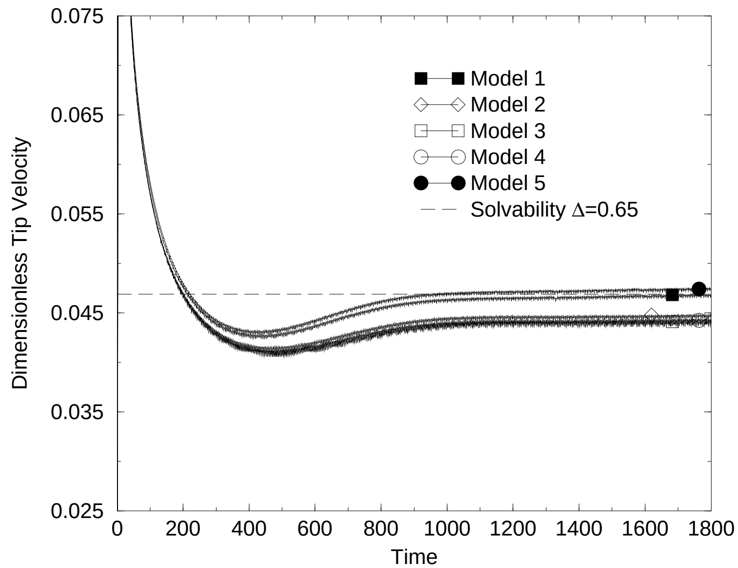

- For too large Δ the asymptotics breaks down because the interface Peclet number $P_i \equiv WV/D$, the expansion parameter, is not small enough.
- We reduced P_i by keeping W the same and increasing d_0, but with Δ kept the same. This corresponds to solving for a different physical system, of course.

IMPROVING PHASE FIELD MODEL ASYMPTOTICS

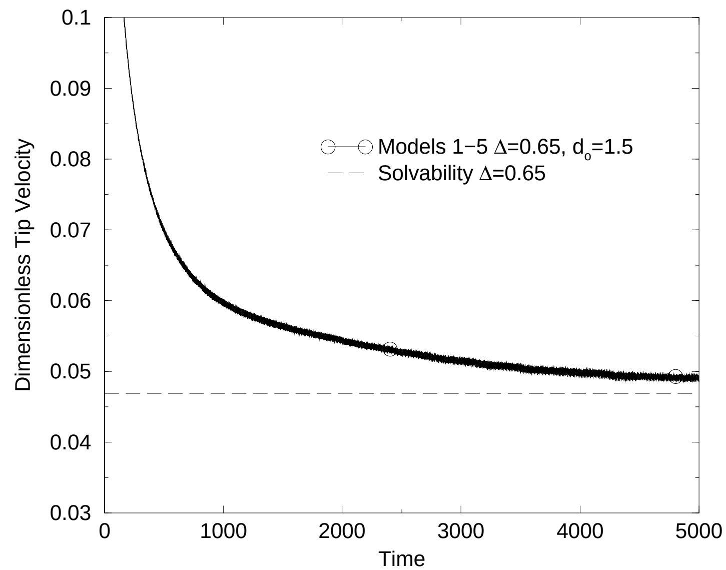

- Keeping Δ fixed but reducing P_i restored agreement.
- In practice, at fixed Δ the only parameter one can vary without changing the actual system being simulated is W, which again leads to costly computation
- Higher order in P_i computations (using RG) are being pursued as a possible alternative

ISOLATED DENDRITE AT LOW UNDERCOOLING

- Both dendrite arms are within thermal boundary layer
- Selection constant σ^* matches solvability theory
- Shape/velocity does not match solvability solution for isolated arm until tips are out of range of each other.

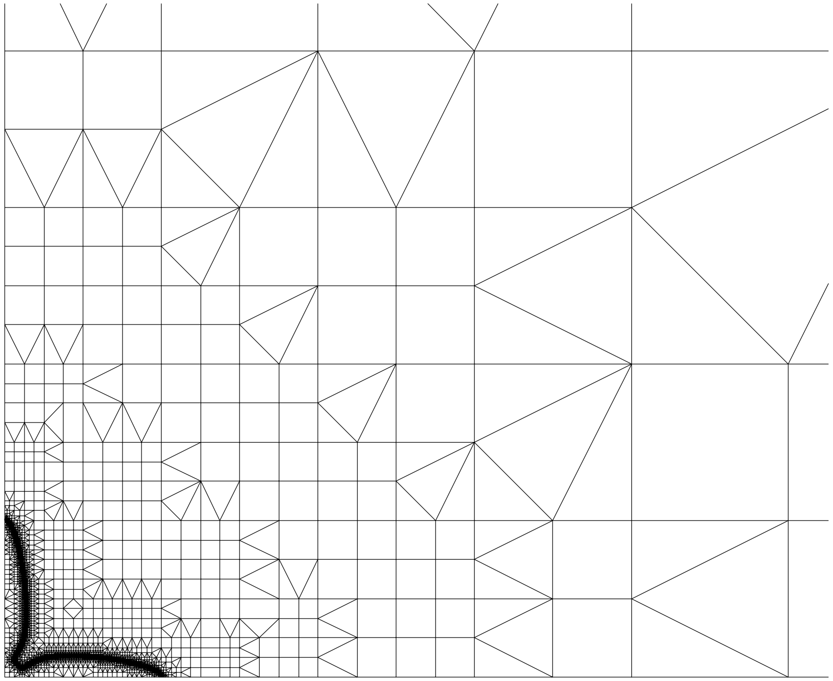

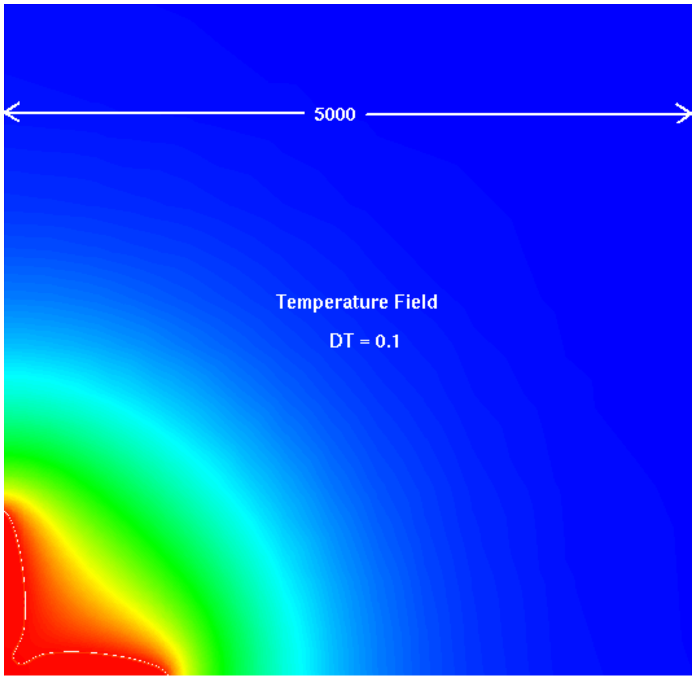

Nigel Goldenfeld

SUMMARY OF RESULTS FROM 2D CALCULATIONS

- At high undercooling, computations match microscopic solvability theory
  - Tip shape
  - Tip velocity
  - Selection constant σ^*
- At low ΔT, dendrite branches interact, violating assumptions
- Tip velocity and shape may never agree between experiments and theory for isolated branch if sidebranches are present
- As long as the $W \to 0$ limit is being taken, the predictions of phase field models are indeed universal. There is no preferred phase field model (as some have argued on thermodynamic grounds).
- Deviations from correct behaviour are observable when the phase field model is used outside its regime of validity. Higher order calculations are needed in this case.

DENDRITE MORPHOLOGY

- Consider *mean* dendrite profile of primary dendrite branch
- Scale global shape by: $\ell \sim (x_{tip} - x_{root})$ and width y_{max}

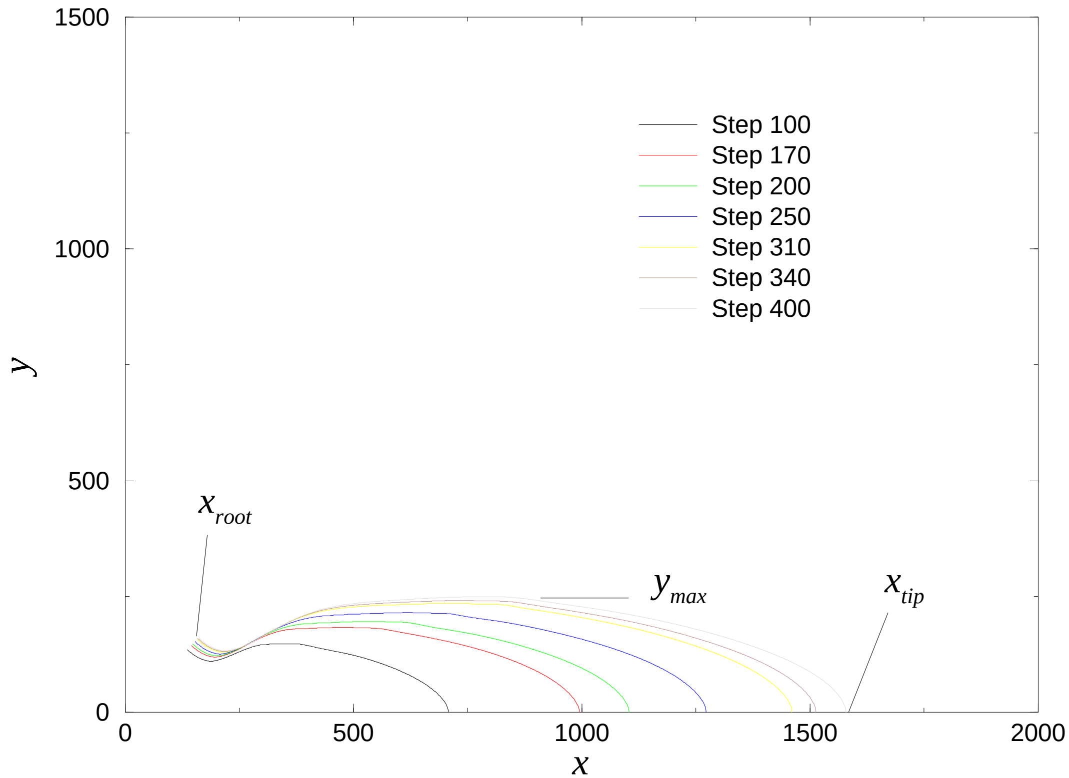

SELF-AFFINITY IN EXPERIMENTAL PIVALIC ACID DENDRITES

- Scale dendrite arm by $\ell \sim (x_{tip} - x_{root})$ and $w \sim y_{max}$
- Self-affinity in global profiles in PVA from USMP-4 experimentl
- Differences at tip due to 2-D computations vs. 3-D experiments

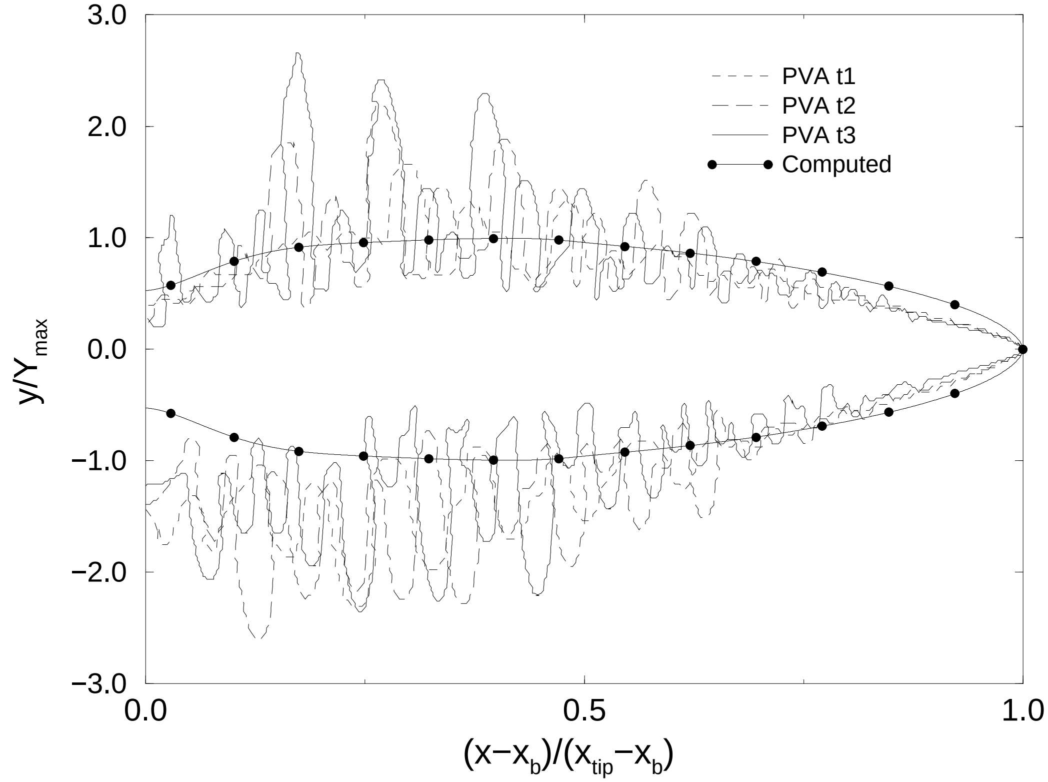

PHENOMENOLOGY: DIRECTIONAL SOLIDIFICATION

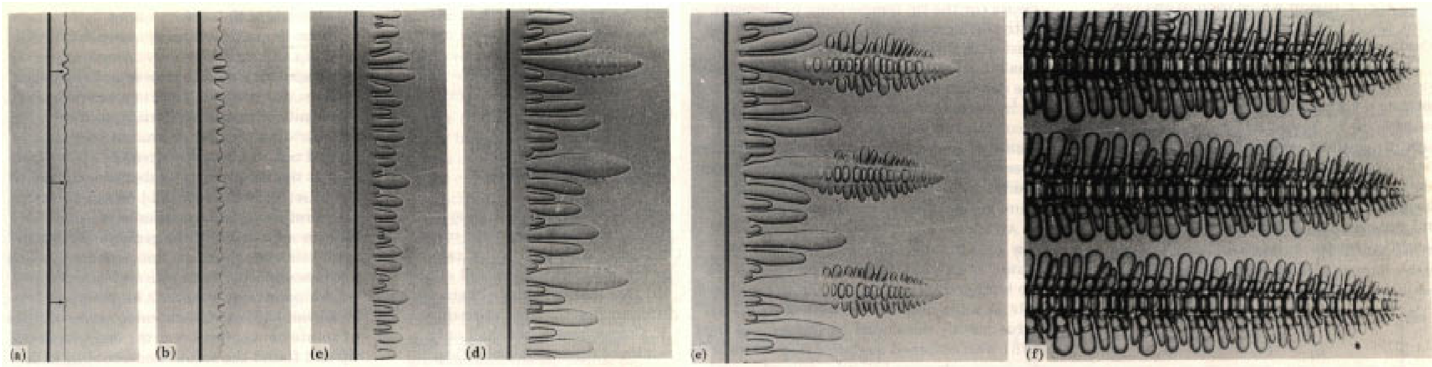

- Ref: Trivedi and Somboonsuk, *Mat. Sci. Eng.*, 1984
- Succinonitrile-acetone alloy growing at constant G and V
- Pattern selection: initial instability to dendrite dimensions
- Primary and secondary dendrite arm spacings

DIRECTIONAL SOLIDIFICATION: THE ISSUES

- Interface unstable, fingers develop, inter-dendrite spacing established
- Pattern selection depends on process parameters: V and G
- Pattern selection *also* dependent on sidebranching and initial conditions
- Computation of *large-scale* solidification microstructures requires large systems, long CPU times:
  - ◇ Computational domain 13066×52150 (units of d_o)
  - ◇ Minimum grid spacing: $\Delta x_{\mathrm{min}} = 3.19 d_o$
  - ◇ $d_o = 6.39 \times 10^{-6}$mm
  - ◇ One CPU-month on Origin or Sun workstation
- Directional solidification invariably involves two-sided diffusion. Must derive the phase field model taking this into account. Basic trick: interface position can be shifted by an amount of $O(W)$ without changing the asymptotics.

PATTERN SELECTION: INTERDENDRITIC SPACING

- Quasi-periodic initial interface configuration $\Rightarrow$ quasi-periodic structure

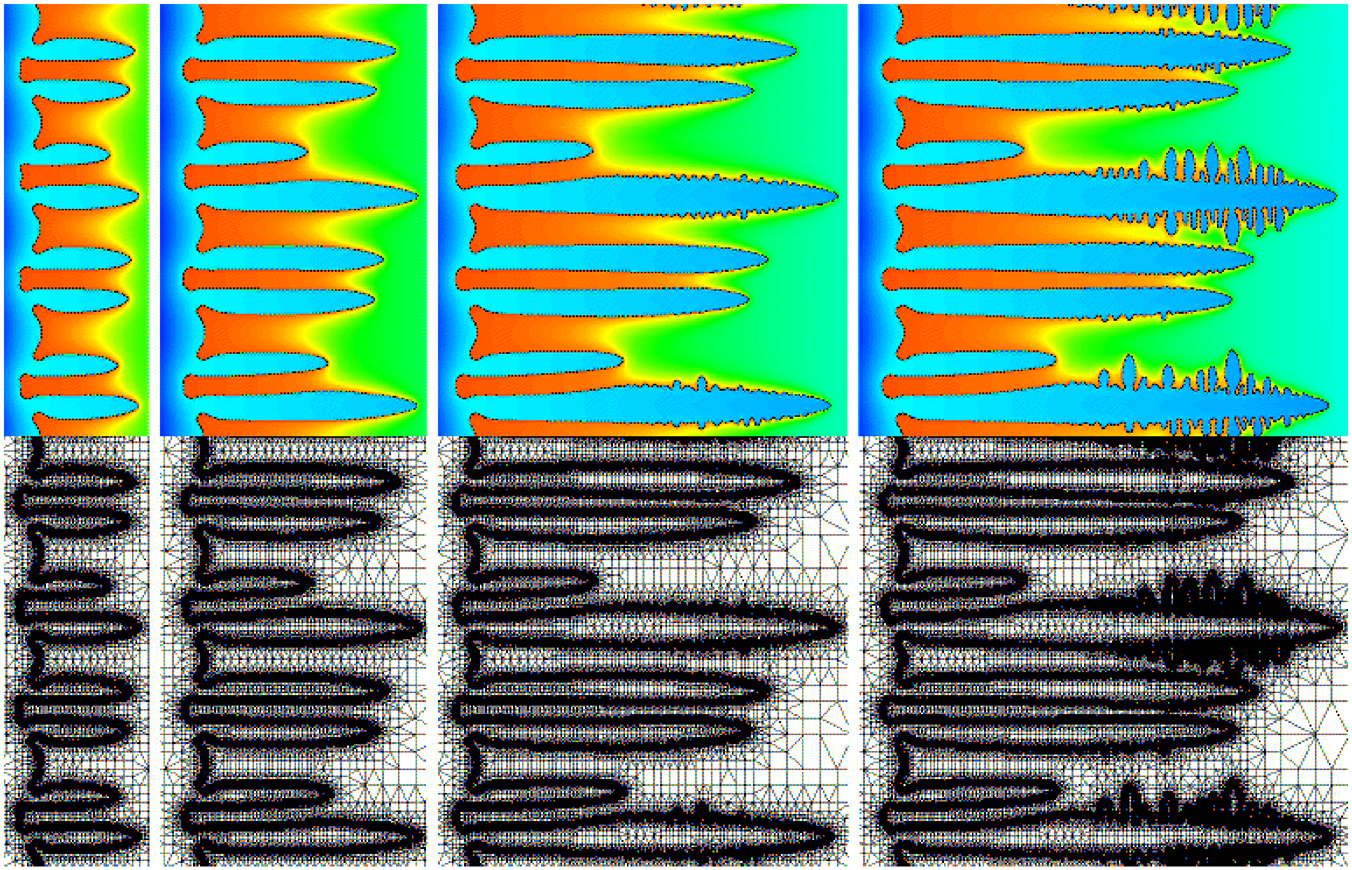

PARALLEL IMPLEMENTATION OF ALGORITHM

- CPU time further reduced by new parallel implementation
  - ◇ Parallelize using OpenMP (shared memory)
  - ◇ Domain decomposition into longitudinal stripes
  - ◇ Node numbering for improved cache performance

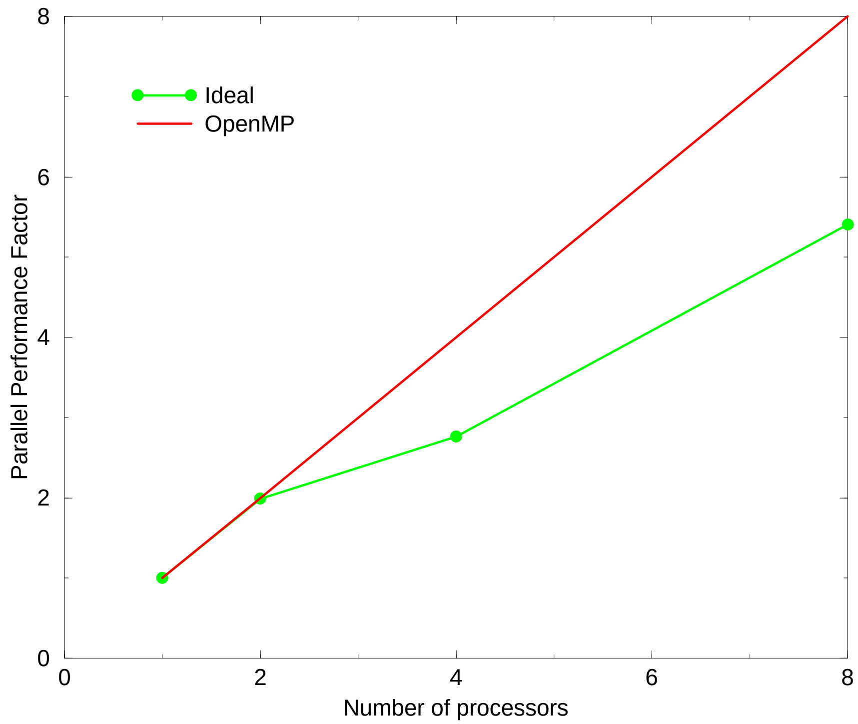

EXPERIMENTS AT DEGENERATE ORIENTATIONS

- Experiments by Bodenschatz, et al on SCN - (poly)ethylene oxide
- Low speed results: 2.71 μm/s and 8.96 μm/s

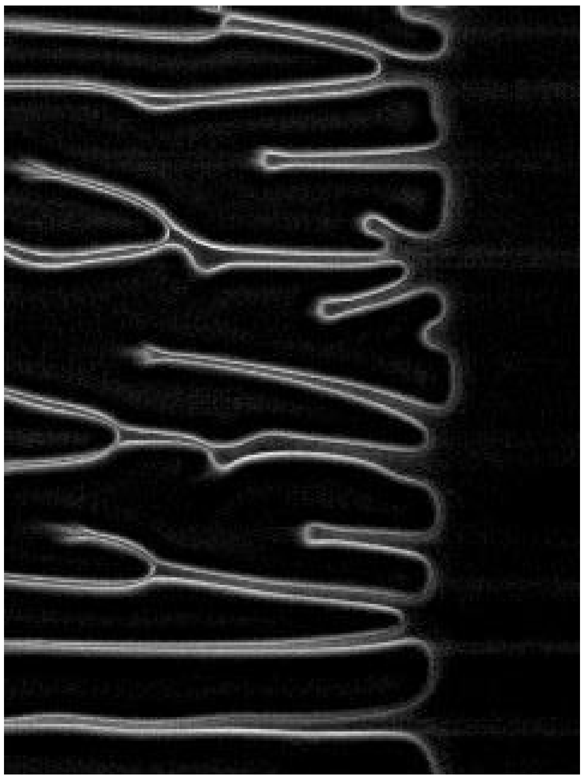

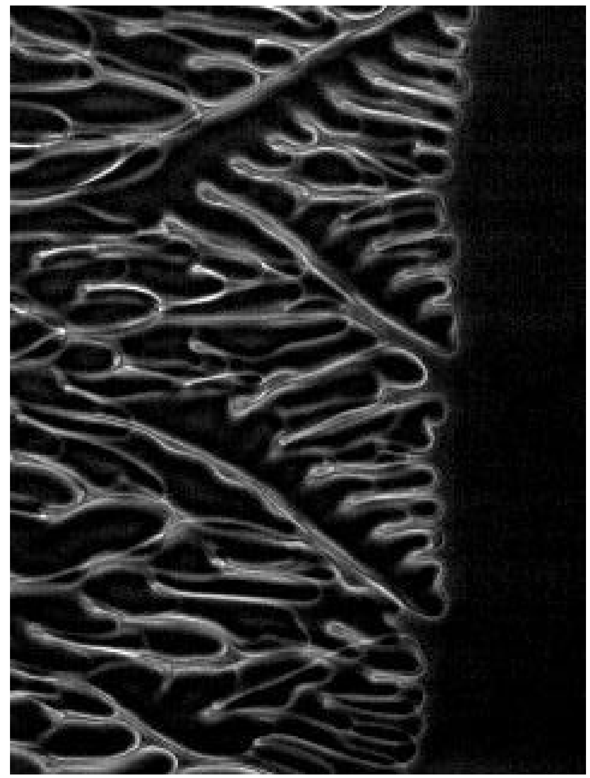

SIMULATION WITH LOW ANISOTROPY

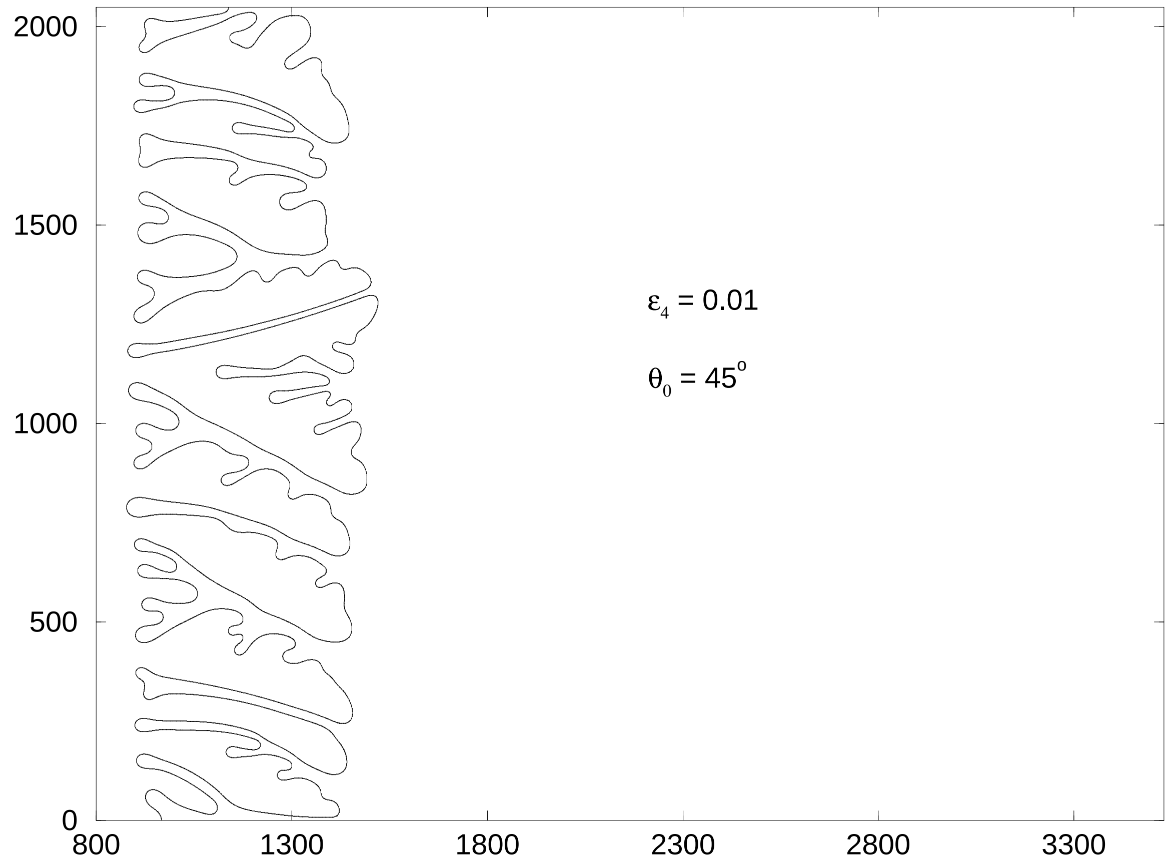

SIMULATION WITH HIGH ANISOTROPY

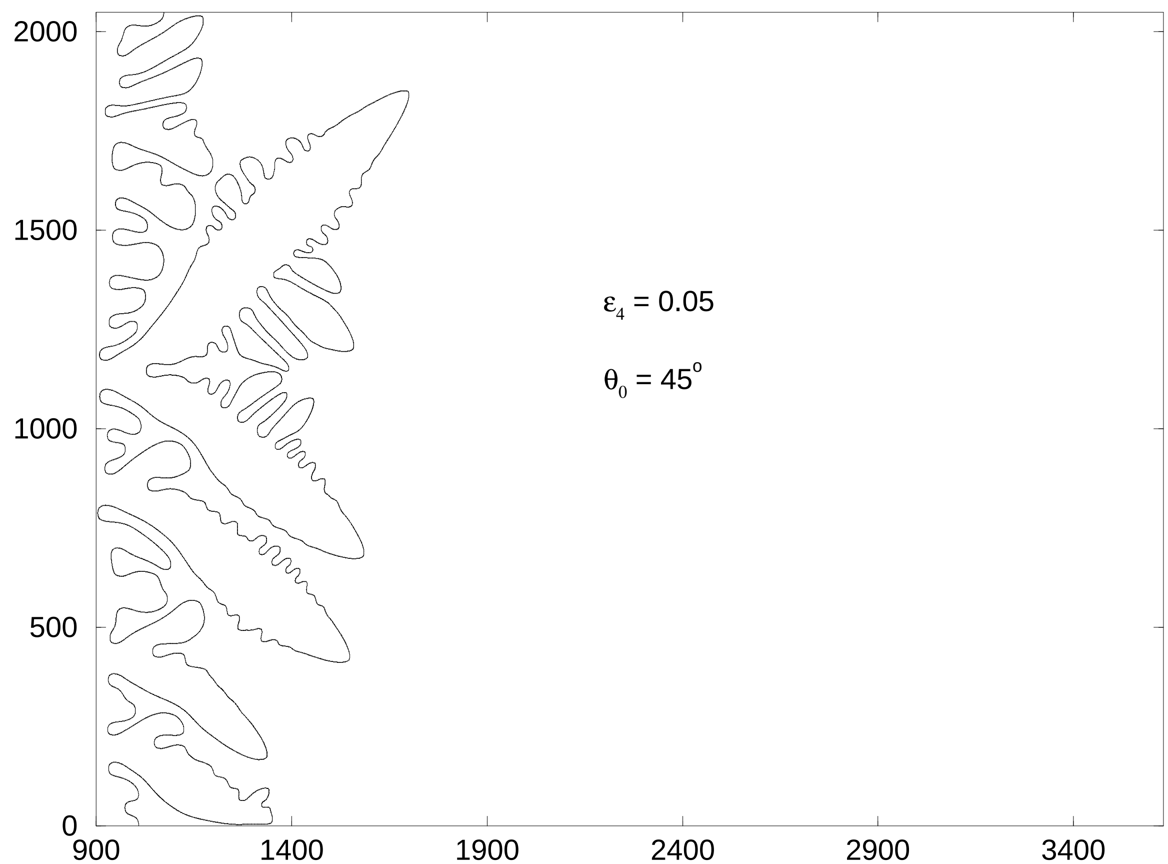

LEVEL SET METHODS

- Phase field models nicely finesse the problem of interface tracking and boundary conditions implementation, but ...
  - ◇ Require solution of a complex asymptotics problem to find the relation between the parameters of the sharp interface model and the phase field model
  - ◇ Require the numerical solution of a stiff PDE
- Level set method follows the evolution of the contour of $\phi(\mathbf{r}) = 0$
- No asymptotics is required as an initial step; equations not stiff
- Discontinuities can be naturally handled
- This contribution: use interpolation schemes to construct the normal velocity. Resulting computations accurate enough to compare with solvability theory and phase field models

LEVEL SET METHODS: ALGORITHM

- Advancing the interface
  - ◇ $\frac{\partial \phi}{\partial t} + F|\nabla \phi| = 0$ where $F = V_n$ at the interface and ϕ is the signed normal distance from the interface (positive in liquid, negative in solid).
  - ◇ Construct F by finding nearest point of interface $\mathbf{x_i}$ to a given grid point $\mathbf{x_g}$: use Gibbs-Thomson boundary condition to determine u_i at the interface: interpolate u away from the interface a distance one lattice spacing and estimate the normal derivatives of u; hence determine F.
  - ◇ **Step 1:** Advance interface using the level set equation with a 5th order weighted essentially nonoscillatory scheme in space and 3rd order Runge-Kutta in time to give a second order in space, first order in time algorithm.

LEVEL SET METHODS: ALGORITHM AND RESULTS

- **Step 2:** Reinitialize to make ϕ again the signed distance function
- **Step 3:** Solve the diffusion equation with Crank-Nicolson but take into account different diffusivities for a stencil that straddles the interface
- Compare phase field and level set for symmetric model $\Delta = 0.55$

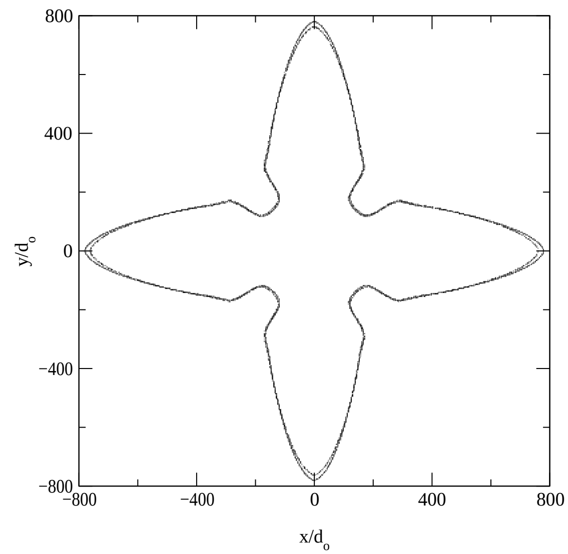

LEVEL SET METHODS: COMPARISON WITH THEORY

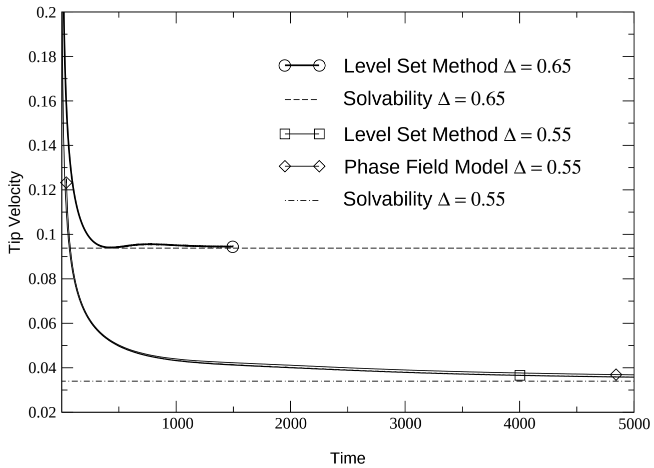

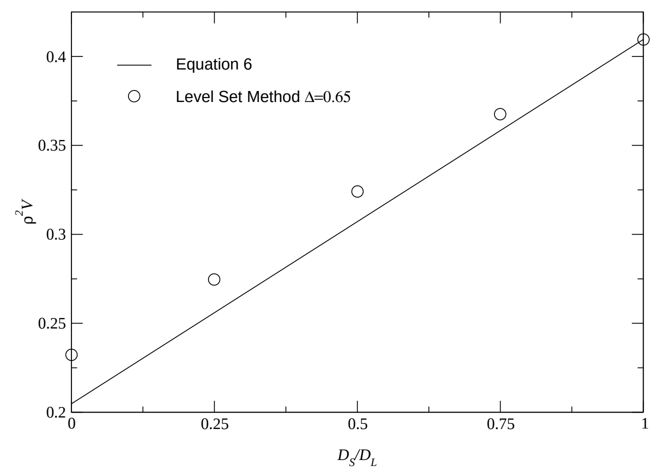

- At long times, the level set code converged to the *steady state* prediction of solvability theory
- The *time dependence* was precisely that of the phase field model under the same initial conditions
- For two-sided case, we found reasonable agreement with heuristic theoretical prediction by Barbieri and Langer

DENDRITIC GROWTH WITH FLUID FLOW

- Heat and solute transport mechanisms

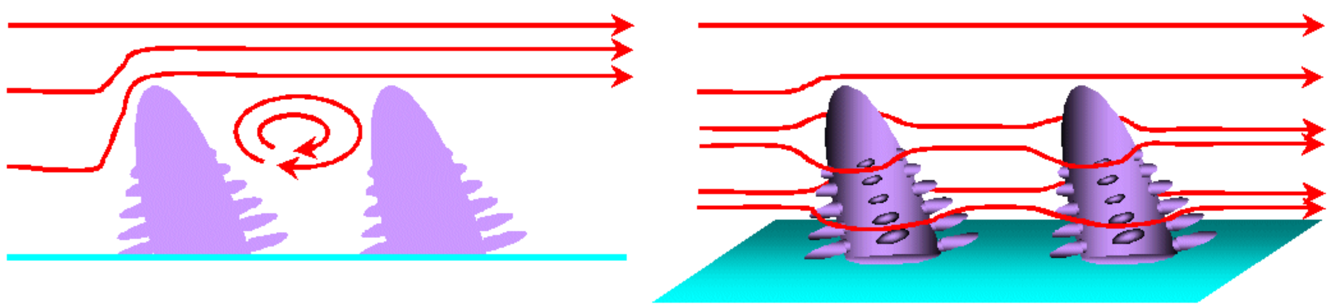

2D 3D

- 2D model: Fluid flows up and over the tip
- 3D model: Fluid flows vertically and horizontally around the tip
- Low Re, high Pe

ADAPTIVE GRID PROCEDURE IN 3D

- Octree data structure
- Disconnected nodes handled by constraints

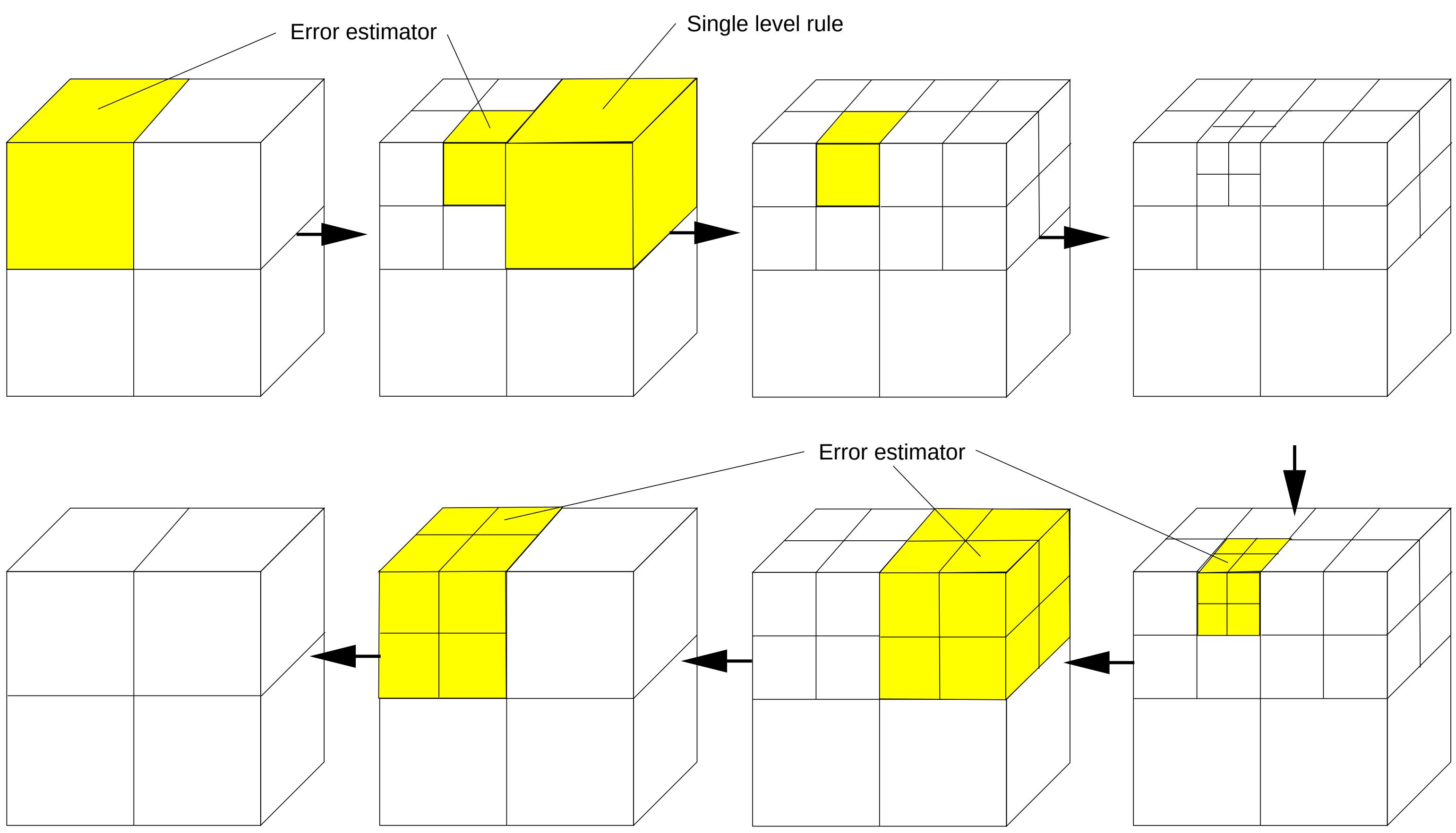

LINEAR CONSTRAINT SCHEME FOR DISCONNECTED NODES

- Disconnected edge mid-node : $V_2 = \frac{V_1+V_7}{2}$, $V_5 = \frac{V_1+V_{11}}{2}$, $V_6 = \frac{V_1+V_9}{2}$
- Disconnected face mid-node : $V_3 = \frac{V_1+V_7+V_8+V_9}{4}$, $V_4 = \frac{V_1+V_{11}+V_{10}+V_9}{4}$
- Modify the elemental stiffness matrix
- Modify the elemental connectivities
  - ◇ [3, 12, 4, 6, 2, 13, 5, 1] $\Rightarrow$ [8, 12, 10, 9, 7, 13, 11, 1]

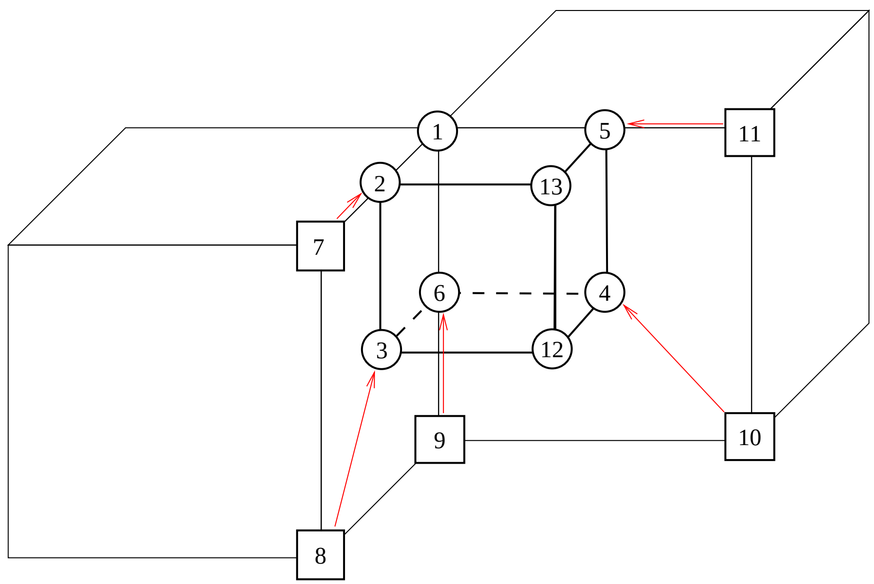

3D DENDRITE GROWTH

- Parameter values:
  - $\Delta = 0.45$, $D = 1$, $\epsilon_4 = 0.04$, $\lambda = 1.600$, $\tau_0 = 0.942$, $\delta = 0.0615$
  - $\Delta x_{min} = 1.6$, $dt = 0.4$, system size = $409.6 \times 409.6 \times 409.6$
- Evolving mesh

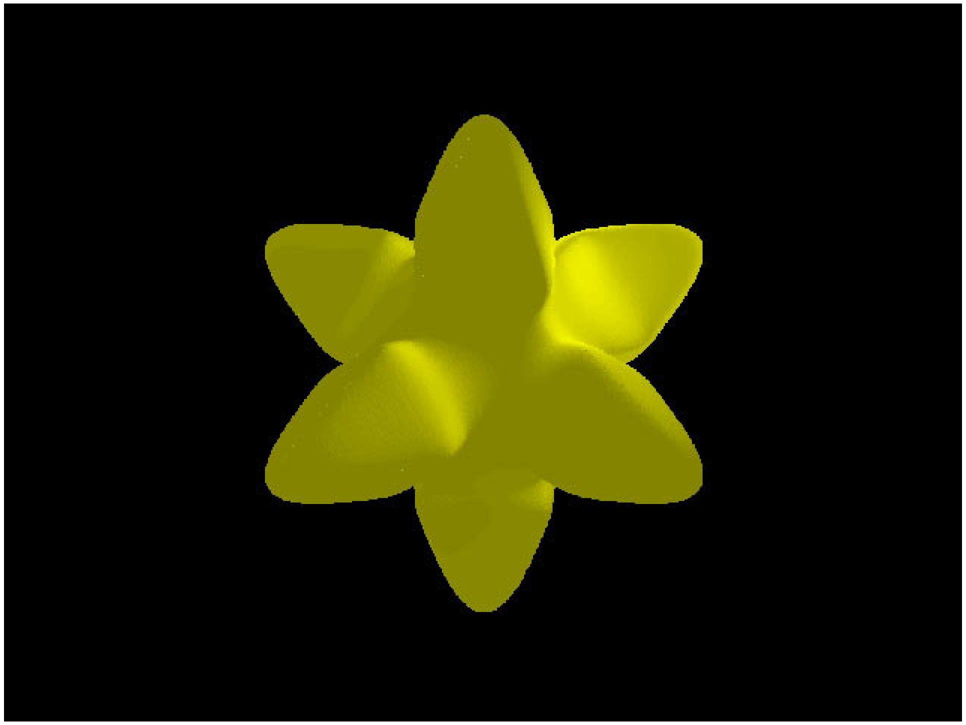

3D DENDRITE GROWTH: GRID DETAILS

- Mesh configuration(t=6720)
  - ◇ Lowest refinement level: 3(Δx=25.6)
  - ◇ highest refinement level: 7(Δx=1.6)
  - ◇ Number of elements: 345,787 number of nodes: 418,520

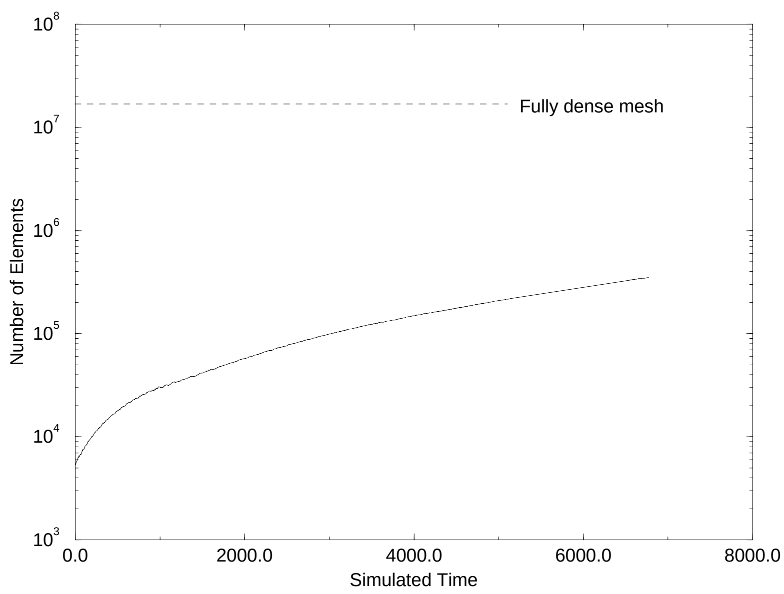

RE-EXAMINE SELF-AFFINITY IN PVA DENDRITES

- Scale dendrite arm by $\ell \sim (x_{tip} - x_{root})$ and $w \sim Y_{max}$
- 3-D envelopes match well to experimental dendrites

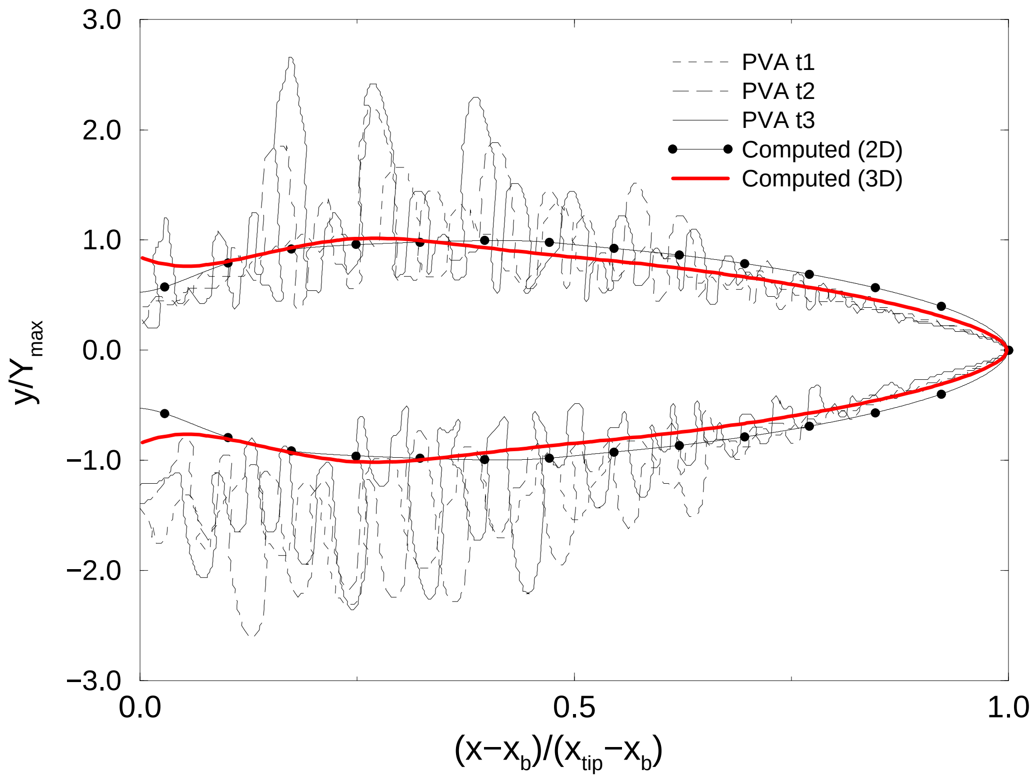

PHASE-FIELD METHOD WITH FLOW

- Mixture approach, following Beckermann et al.
- Continuity

$$\nabla \cdot \left[\frac{1-\phi}{2} \mathbf{u} \right] = 0$$

- The averaged momentum equation:

$$\frac{D}{Dt}\left[\left(\frac{1-\phi}{2}\right)\mathbf{u}\right] = -\left(\frac{1-\phi}{2}\right)\nabla p + \nu \nabla^2 \left[\left(\frac{1-\phi}{2}\right)\mathbf{u}\right] - \nu \frac{h^2(1-\phi^2)}{4\delta^2}\mathbf{u}$$

- The averaged energy equation with $\theta = c_p(T - T_m)/L_f$:

$$\frac{\partial \theta}{\partial t} + \left(\frac{1-\phi}{2}\right)\mathbf{u} \cdot \nabla \theta = D \nabla^2 \theta + \frac{1}{2}\frac{\partial \phi}{\partial t}$$

PARALLEL IMPLEMENTATION OF 3D CODES

- Need higher speedup factors ($\mathcal{O}(100)$)
- Domain decomposition not obvious
- Strategy
  - ◇ Distributed memory
  - ◇ CHARM++
- Code details
  - ◇ Explicit time stepping for phase-field, implicit for others
  - ◇ Flow computed using semi-implicit approximate projection method
  - ◇ Element-by-element conjugate gradient solver

FRAMEWORK FOR PARALLELIZATION BY CHARM++

Subroutine "INIT"

- Preprocessing
- Create an adapted grid
- Domain partition by METIS

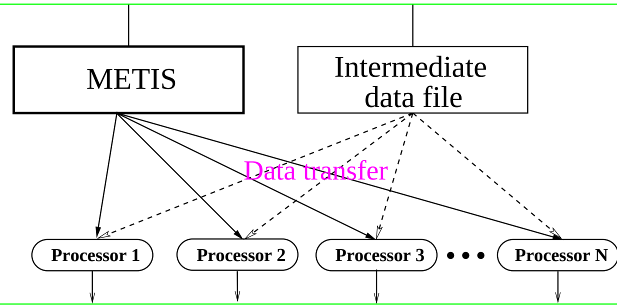

Subroutine "DRIVER"

- Call "FEM_create_FIELD (register the memory allocation size and offset)
- Loop for iterative solver
  - Loop for assembling the nodal values
  - Call "FEM_Update_Field" (combine values at shared nodes)
  - Call "FEM_Reduce" (sum errors from all nodes)

Subroutine "FINALIZE"

- Merge subdomains into global domain
- Postprocessing

PARALLEL PERFORMANCE OF CODE

- Performs 100 time steps on a single mesh

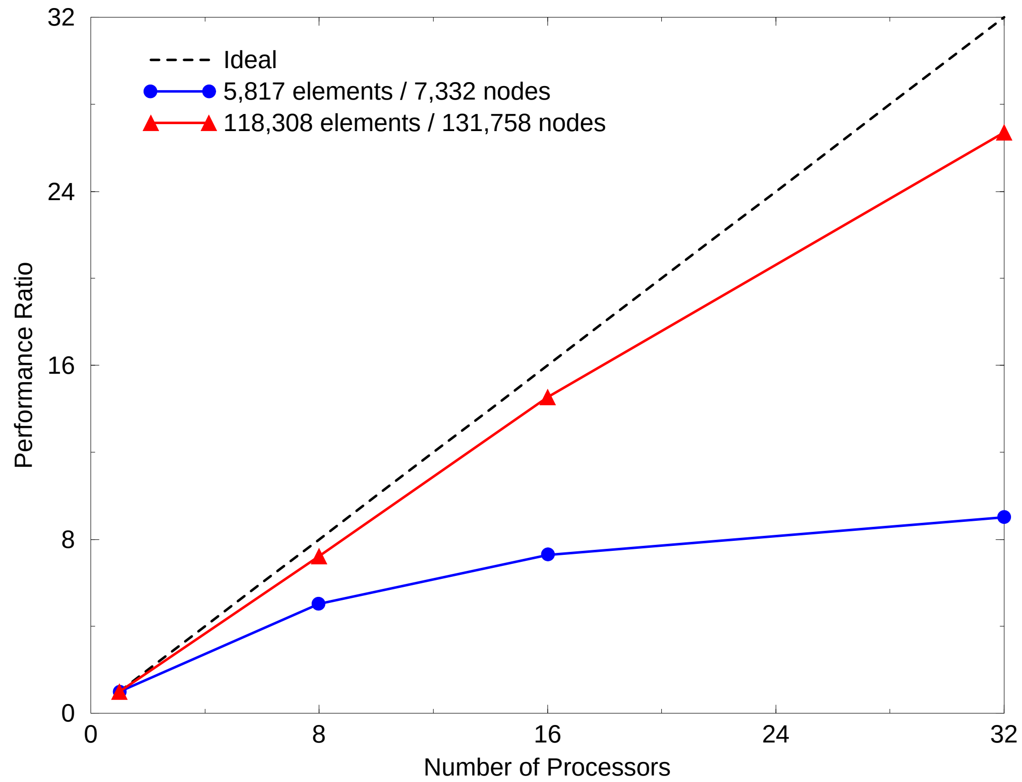

3D DENDRITE GROWTH: WITH AND WITHOUT FLUID FLOW

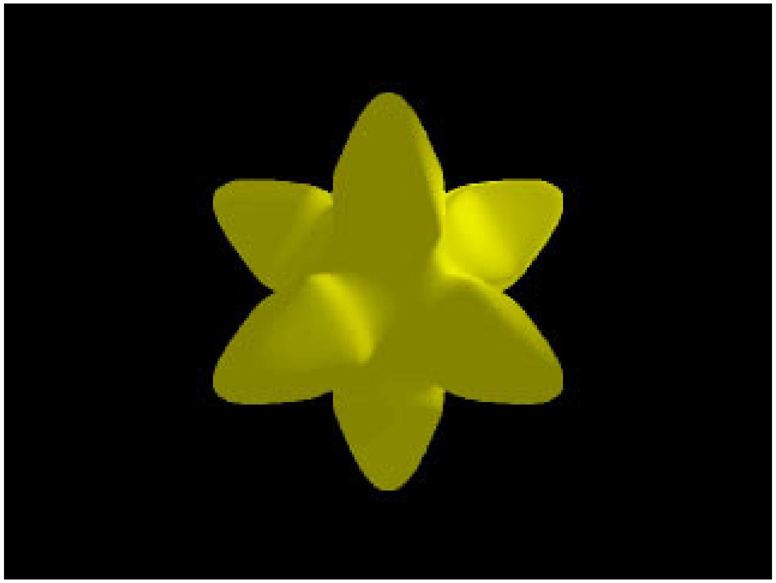

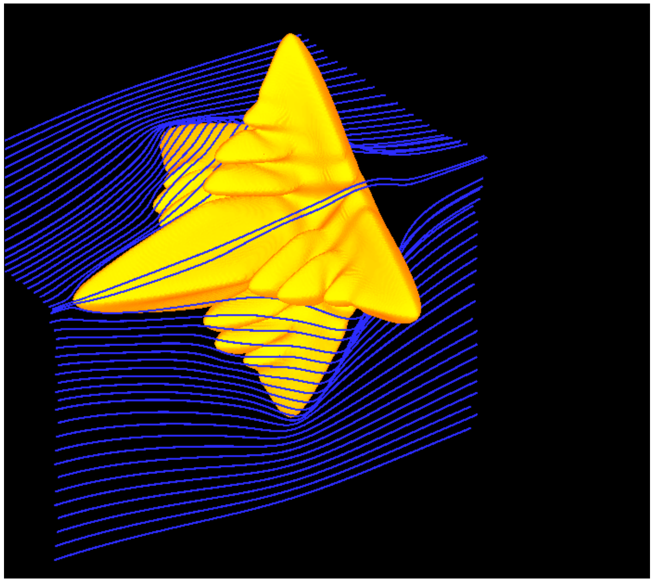

3D DENDRITIC GROWTH WITH FLUID FLOW

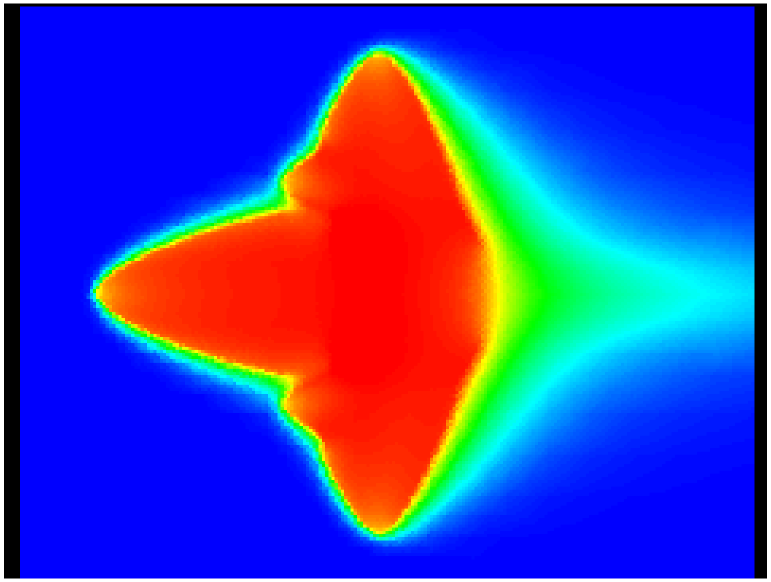

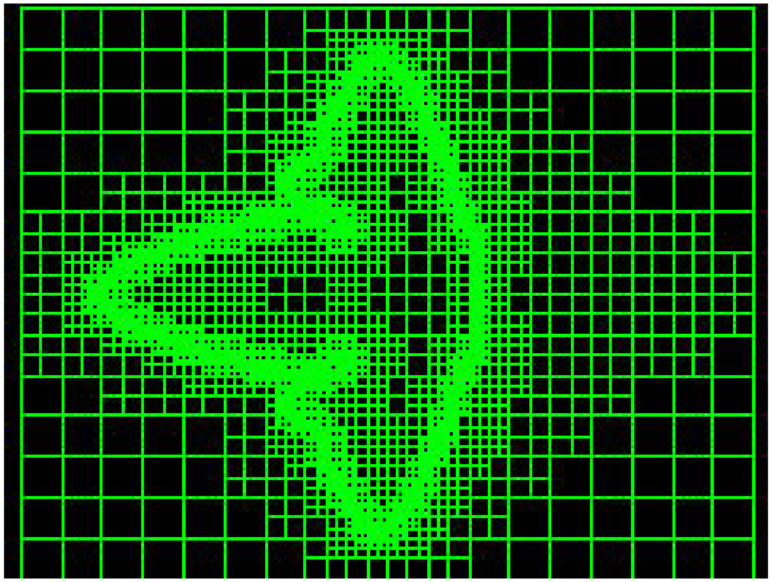

EFFECT OF ORIENTATION

- Flow parallel to $< 110 >$

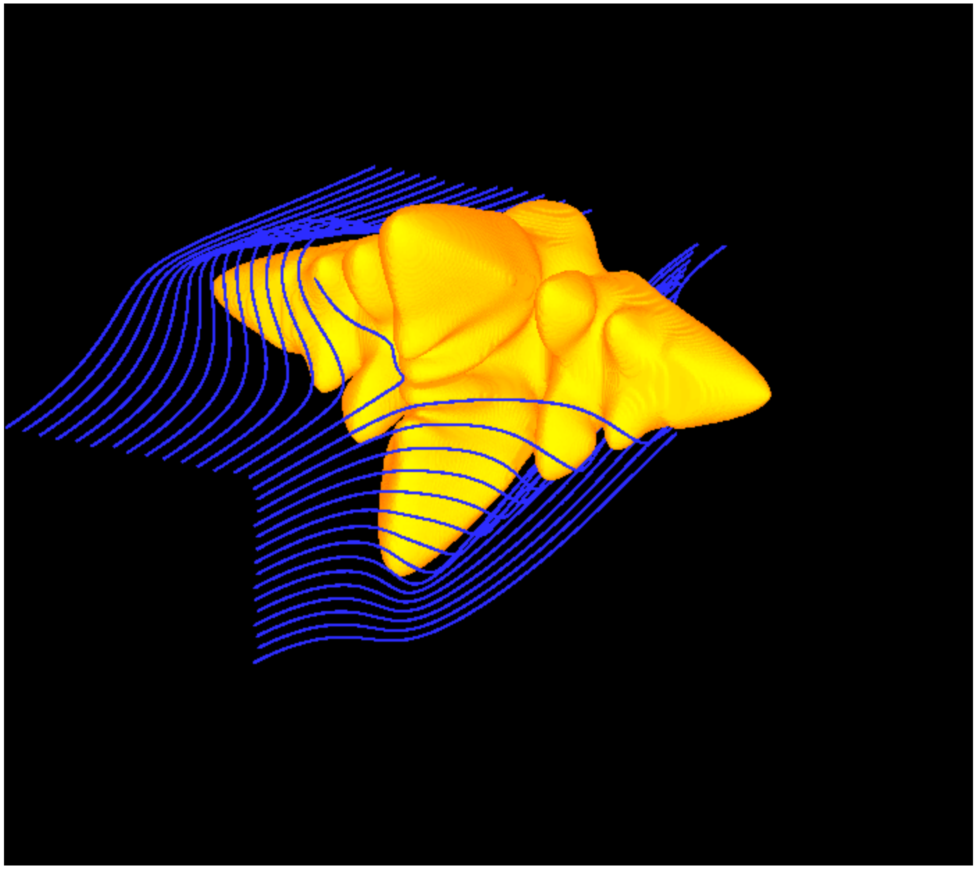

CONCLUSION

- Dendritic growth is complex pattern selection problem
- Numerical simulations can provide realistic tests of theory
- Computations take too long to be done sequentially
- Adaptive, 3-D Navier-Stokes, phase field code
- Enables comparison to experimental observations